Erzincan Üniversitesi
Fen Bilimleri Enstitüsü Dergisi
2018, 11(2), 138-148

Erzincan University
Journal of Science and Technology
2018, 11(2), 138-148

ISSN: 1307-9085, e-ISSN: 2149-4584 DOI: 10.18185/erzifbed.356654

Neuro-Wavelet Based Critical Firing Angle Determination of Phase Controlled DC Motor Drive

Mehmet Zeki BİLGİN

Kocaeli University, Faculty of Engineering, Department of Electrical Engineering, İzmit/Kocaeli

Geliş / Received: 21/11/2017, Kabul / Accepted: 09/07/2018

Abstract
In this work, a Neuro-Wavelet Network (NWN) based method is proposed to calculate the critical triggering angle of DC motor fed by the three phase controlled rectifier. Firstly, the critical triggering angles for DC motor drive system are computed at different operation conditions. Afterwards, the NWN is trained with this data. The critical triggering angle is derived from NWN for any operation condition. The several simulation examples have been given to illustrate the performance and effectiveness of the proposed method. The simulation results of the drive system show that the critical firing angle is determined precisely with the NWN.

Keywords: Neuro-Wavelet Networks, Phase Controlled DC Motor Drive, Critical Triggering Angle, Discontinuous Current Conduction

Dalgacık-Sinir Ağı Yaklaşımı ile Faz Kontrollü DC Motor Sürücülerinde Kritik Tetikleme Açısının Belirlenmesi

Öz
Bu çalışmada Dalgacık Sinir Ağı (DSA) yaklaşımı ile üç fazlı kontrollü doğrultucu ile beslenen DA motorlar için kritik tetikleme açısının belirlenmesi önerilmiştir. İlk olarak farklı çalışma durumlarında kritik tetikleme açıları hesaplanmıştır. Sonrasında DSA bu veriler ile eğitilmiştir. Herhangi bir çalışma durumu için kritik tetikleme açısı DSA' dan üretilmektedir. Benzetim çalışması ile önerilen yöntemin etkinliğini belirlenmiştir. Sürücü sistemin benzetim sonuçları, kritik tetikleme açısının DSA ile kesin bir şekilde hesaplanacağını göstermektedir.

Anahtar Kelime: Dalgacık Sinir Ağı, Faz Denetimli DC Motor Sürücü, Kritik Tetikleme Açısı, Süreksiz Akım Çalışma

1. Introduction

DC motors are not commonly used in industry but the specific DC motors such as Permanent magnet DC motors are used in some specific applications with drive systems (Naresh and Triphati, 2016; Jiang et al., 2017; Joshi et al., 2017). DC motor drive systems generally use two types of power converters. These are DC Choppers and Phase Controlled Converters (Kundu et al., 2017). In this work, the motor is driven with three phase controlled AD/DC converter. Since the electromagnetic torque is produced by armature current with nominal field current, the electromagnetic torque waveform of DC motor is very similar to armature current in shape. The minimization of the current ripple is important for constant torque requirement (Guru and Hızıroğlu, 2001).

If the armature supplies from one-phase controlled rectifier the motor current has ripple. Therefore, the electromagnetic torque has also ripple and changes over time. These torque ripples are not desired in special applications. Since the minimization of the torque ripple the three phase controlled rectifier can be used. The ripple can be reduced partly with this converter. But the DC motor current can be continuous or discontinuous mode according to the firing angle of the converter. If the current is discontinuous the torque has ripple. Thus, the motor should not be operated at

*****Correspondence to: bilgin@kocaeli.edu.tr

discontinuous mode. There is a critical firing angle for any operation point. This critical angle must be calculated prior to use.

In the past years, active research has been carried out in neural network control (Abulafya, 1995; Verma et al., 2017; Azman et al., 2017; Son et al., 2017; Omidvar and Elliott, 1997, Narendra and Campagna, 1990). The characteristics of fault-tolerance, parallelism and learning suggest that they may be good candidates for implementing real-time adaptive control for nonlinear dynamical systems (Nahavandi et al., 2018; Popov et al., 2018; Kurnia et al., 2017; Guney et al., 2017; Singh et al., 2017). It has been proven that artificial neural network can approximate a wide range of nonlinear functions (Khosravi et al., 2017; Kumar et al., 2017; Karas and Kozak, 2018; Dmytro et al., 2018). Recently, wavelets have become a very active subject in research area. Especially, wavelet neural networks (WNN) inspired by both the feed-forward networks and wavelet decompositions have become a popular tool for function approximation (Prema et al., 2015; Lin and Shieh, 2002; Isa et al., 2017; Rabiah and Saad 2016; Sridhar et al.,2015; Hafidz et al., 2017).

In this paper, the determination of the critical firing angle using Wavelet Neural Networks (WNN) for DC motor fed by three phase controlled rectifier has been carried out. The remaining sections of the paper was organized as follows. Section 2 describes the DC motor drive systems. In Section 3, the drive system was analyzed in details. In Section 4, The Neuro-Wavelet Network structure was described. The simulation results of proposed system was given in Section 5. Finally, Section 6 is the conclusion for this research.

2. The DC Motor Drive System

A typical DC motor drive system is shown in Fig.1.

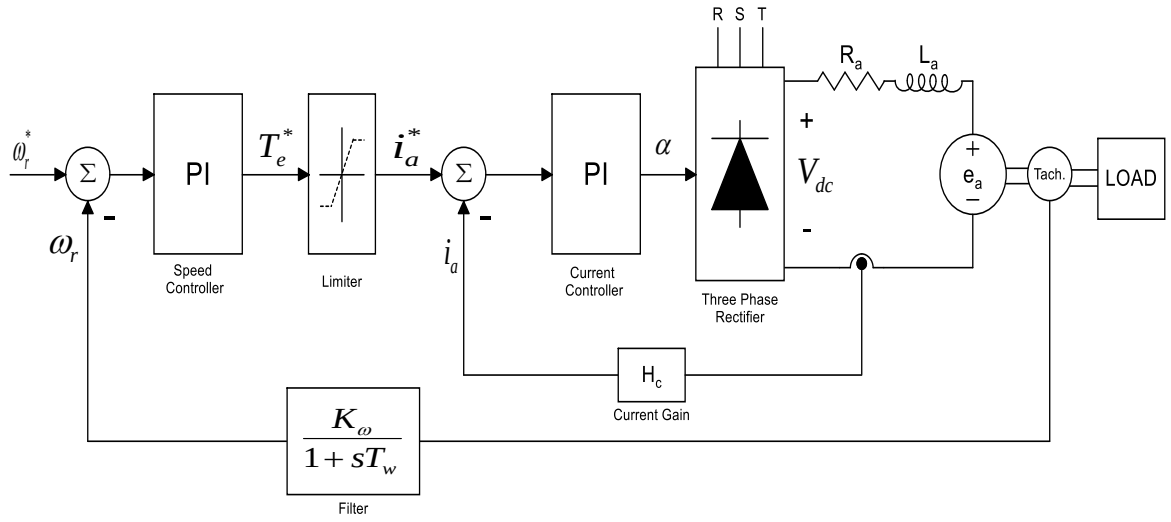

Figure 1. Phase controlled DC motor drive system.

The system consists of four main parts. These parts are the DC motor, the phase controlled rectifier, the load and the controller.

2.1. Three Phase Controlled Converter

The three phase controlled converter output voltage can be changed by delaying the firing signals. The delay is introduced in the form of triggering signals to the gates of the thyristors. The delay angle is generally named α. The motor terminal voltage can be changed during the start-up or speed control. Thus, the output voltage of the converter should also be changed. A typical three phase controlled bridge converter is shown in Fig.2.

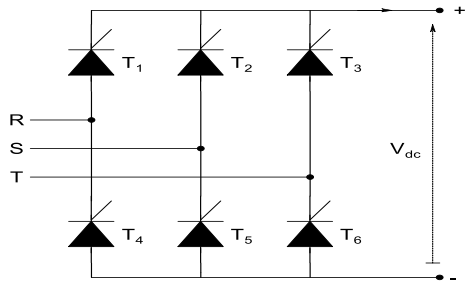

Figure 2. A three phase controlled bridge converter.

The converter output voltage can be adjusted to desired value by changing firing angle α. The average output voltage (V_{dc}) of converter that shown in Fig. 2 is derived as below.

$$V_{dc} = \frac{3}{\pi} V_m Cos(\alpha) \qquad (1)$$

where V_m is the peak value of the input voltage.

2.2. Mathematical Model of DC Motor and Load

It is well known that the equivalent circuits of separately excited DC motor can be drawn as Fig.3. The armature winding has a resistance R_a and a self inductance L_a. V_a, e_a and I_a are supply voltage, induced emf and armature current, respectively.

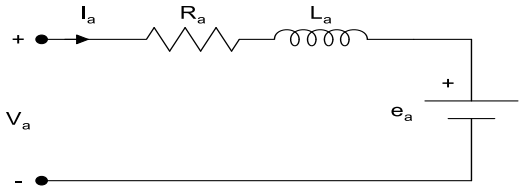

Figure 3. Separately excited DC motor equivalent circuit.

The terminal voltage relationship is written as (2) from Fig. 3.

$$V_a = e_a + i_a \cdot R_a + L_a \frac{di_a}{dt}$$
$$e_a = K_b \cdot \omega_r \qquad (2)$$

The state-space form dynamic equations of DC motor are written as,

$$\frac{di_a}{dt} = -\frac{R_a}{L_a} \cdot i_a - \frac{K_b}{L_a} \cdot \omega_m + \frac{V_a}{L_a}$$
$$\frac{d\omega_m}{dt} = \frac{K_b}{J} \cdot \omega_m - \frac{1}{J} \cdot T_L \qquad (3)$$

where J, B, K_b, T_L are the rotor inertia, rotor friction coefficient, emf constant and load torque, respectively.

3. Analysis of Drive System

A three phase thyristor controlled converter with DC motor equivalent circuit is shown in Fig.4.

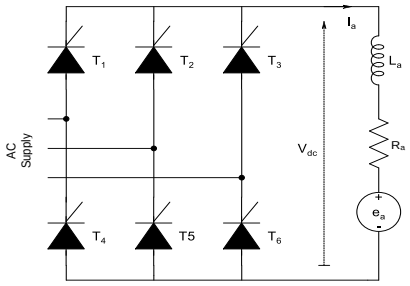

Figure 4. DC Motor equivalent circuit fed by three phase controlled converter.

The average output voltage (V_{dc}) depends on the firing angle. It has oscillatory waveform. Fig. 5 and Fig. 6 show the output voltages and currents for α=30° and α=60°, respectively.

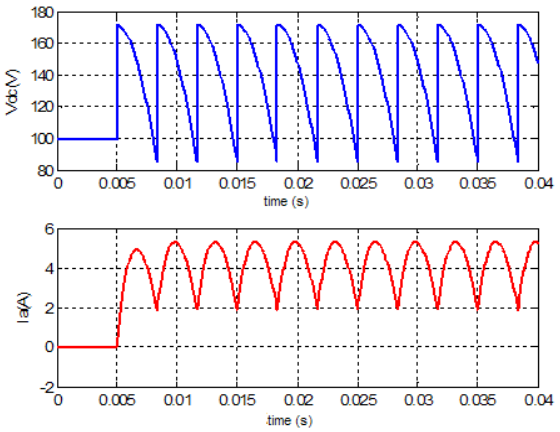

Figure 5. Continuous current condition (α=30°).

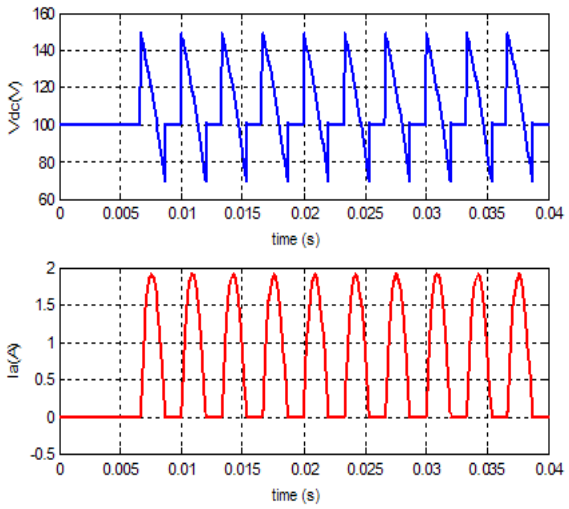

Figure 6. Discontinuous current condition (α=60°).

The armature current of DC motor is shown as continuous form in Fig 5, and discontinuous form in Fig. 6. The period of the V_{dc} is π/3 radian and the output voltage expression is written as;

$$V_{dc} = V_m Sin(\omega_s t + \frac{\pi}{3} + \alpha), \quad 0 < \omega_s t < \frac{\pi}{3} \qquad (4)$$

The DC motor armature current can be continuous or discontinuous depending on the firing angle, while the other factors are constant. However, the armature current must be continuous for constant torque operation. If the armature current is discontinuous, the torque will be also discontinuous. Therefore, the produced torque will be zero over some time period. This is not a desirable effect for the high sensitive applications such as machine tools and robotics. Therefore, the discontinuous current mode should be prevented. The factors of discontinuous mode are identified by using motor equivalent circuit and converter output voltage expression. If the field flux is constant, then the induced emf becomes proportional to the rotor speed, and the terminal relationship is written as

$$V_{dc} = R_a i_a + L_a \frac{di_a}{dt} + K_b \omega_m \qquad (5)$$

Induced emf e_a is constant at constant speed and field flux. This emf is named E. As Krishnan (2001) shows, $i_a(t)$ is obtained by substituting (4) into (5).

$$i_a(t) = \left(\frac{V_m}{|Z_a|}\right)\left\{Sin(\omega_s t + \frac{\pi}{3} + \alpha - \varphi) - Sin(\frac{\pi}{3} + \alpha - \varphi)e^{-\frac{t}{\tau_a}}\right\} - \left(\frac{E}{R_a}\right)\left(1 - e^{-\frac{t}{\tau_a}}\right) + i_{a_0} \cdot e^{-\frac{t}{\tau_a}} \qquad (6)$$

where $\omega_s=2\pi f$ $\varphi=\text{atan}(\omega_s L_a/R_a)$, $\tau_a=L_a/R_a$, $Z_a=R_a+jX_a$ and $E=K_b\omega_m i_{a0}$ and V_m are the initial current at t=0 and peak value of the phase voltage, respectively. i_{a0} is calculated to enter the given initial condition using (6). The period of i_a is π/3. i_a can be written as,

$$i_a(\omega_s t) = i_a(\omega_s t + \frac{\pi}{3}), \quad \cdots$$

$$i_a(\frac{\pi}{3\omega_s}) = i_{a0}$$

Therefore, the initial current expression can be derived as,

$$i_{a0} = \frac{1}{1 - e^{-\frac{\pi}{3\omega_s \tau_a}}} \cdot \left\{\frac{V_m}{|Z_a|} \cdot \left[Sin\left(\frac{2\pi}{3} + \alpha - \varphi\right) - Sin\left(\frac{\pi}{3} + \alpha - \varphi\right)e^{-\frac{\pi}{3\omega_s \tau_a}}\right] - \frac{E}{R_a}\left(1 - e^{-\frac{\pi}{3\omega_s \tau_a}}\right)\right\} \qquad (7)$$

By examining the Eq.7, it is shown that the i_{a0} is related to rotor speed (ω_s), terminal voltage (V_m), L_a (or φ), induced emf (E) and firing angle (α). The triggering angle converting continuous armature current into discontinuous armature current is called critical triggering angle. It can be calculated by assigning the initial armature current i_{a0} to zero in (7). This is given as Krishnan (2001).

$$\alpha_c = \varphi + Cos^{-1}\left\{\frac{\frac{E}{V_m}}{a_3} \cdot \frac{1}{Cos\varphi} \cdot \left(1 - e^{-\left(\frac{\pi}{3\tan\varphi}\right)}\right)\right\} - \frac{\pi}{3} + a_4$$

$$a_1 = \frac{\sqrt{3}}{2}$$

$$a_2 = \frac{1}{2} - e^{-\left(\frac{\pi}{3\tan\varphi}\right)} \qquad (8)$$

$$a_3 = \sqrt{a_1^2 + a_2^2}$$

$$a_4 = \tan^{-1}\left(\frac{a_2}{a_1}\right)$$

This expression shows that the critical triggering angle is a function of the emf, line to line AC voltage and impedance angle (φ)

of the DC motor. The input voltage is generally constant and the α_c only depends on two variables, φ and E/V_m. The critical firing angle versus E/V_m for various value of φ is shown in Fig. 7.

For the continuous current operation, the firing angle α should not exceed the critical firing angle α_c. If α exceeds α_c, the discontinuous current mode occurs. As it can be seen from (8), the firing angle determination can be difficult in case of using on-line operations.

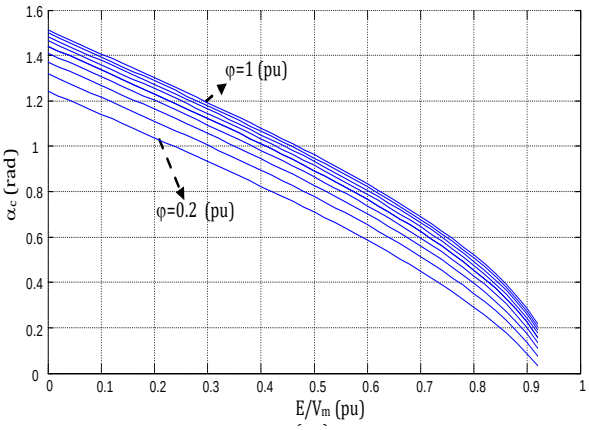

Figure 7. The critical triggering angle versus E/V_m for various value of φ.

In the proposed method, the critical firing angle is derived by using NWN in on-line operation without any calculation from Eq. (8).

4. The Neuro-Wavelet Network

The wavelet networks are developed by the joining the wavelet theory and neural networks. Wavelet networks are feed-forward neural networks and have wavelets activation function. Wavelet functions and neural networks are combined in different styles. One of the applications of neuro-wavelet networks is function estimation.

Given a series of observed values of a function, a wavelet network can be trained to learn the composition of that function, and hence calculate an expected value for a given input. A wavelet neural network usually consists of a feed-forward Artificial Neural Network (ANN) with one hidden layer. It uses nonlinear wavelet functions instead of nonlinear sigmoid or tanh functions.

The structure of NWN is shown in Fig. 8 (Lin et al., 2007; Lin et al., 2004; Khan and Rahman (2010) and it is similar to the ANN. The wavelet networks also consist of an input layer, a hidden layer, and an output layer.

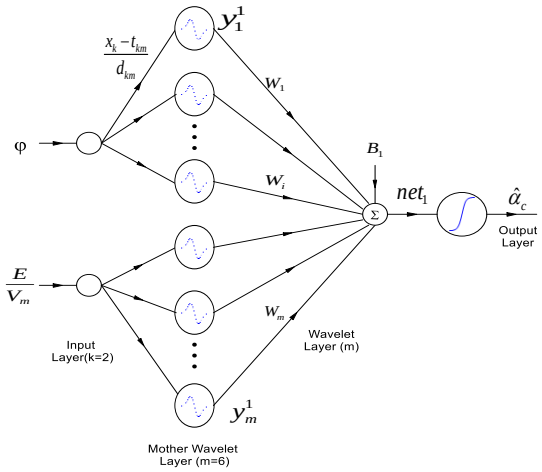

Figure 8. Structure of the Wavelet-neural Network.

The wavelet network model shown in Figure 8 consists of three layers. The first layer is input layer and the number of input neurons is equal to the number of input variables. Here, it has two inputs (φ, E/V_m). The input neurons are connected to the next layer of neurons called mother wavelet layer. The activation functions of this layer neurons are wavelet functions and connected to the third layer, which is called wavelet layer. The fourth layer is output layer which has one neuron with logarithmic sigmoid function. Its output is critical firing angle α_c.

There are many varieties of wavelets function, which can be used in Wavelet-neural Networks. In this study, the first derivative of Gaussian function is used as a mother wavelet function(Φ).

$$\Phi(x) = -x \cdot e^{-\frac{1}{2}x^2} \qquad (9)$$

The output of the mother wavelet layer y_m^1 is then constructed by translating and dilating the mother wavelet Φ according to (10) (Parasuraman and Elshorbagy 2005).

$$y_m^1 = \Phi\left(\frac{x_k - t_{mk}}{d_{mk}}\right) \qquad (10)$$

where t_{mk}, and d_{mk} represents the translation and dilation factors of the wavelet

respectively. The first derivative Gaussian mother wavelet with different translation and dilation factors is shown in Fig. 9. (Parasuraman and Elshorbagy, 2005).

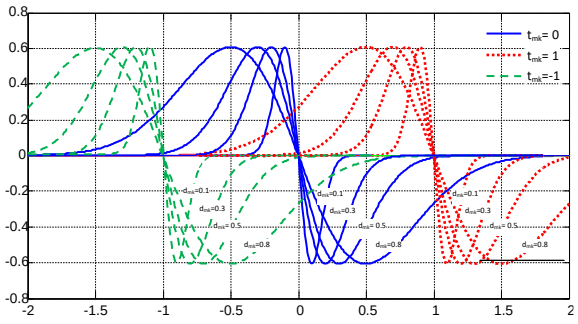

Figure 9. Wavelets with varying dilation and varying translation factors.

The output of wavelet layer is;

$$net_1 = B_1 + \sum_{i=1}^{m} W_i y_i^1 \qquad (11)$$

and the output from the output layer can be represented as

$$\alpha_c = \frac{1}{1+e^{-net_1}} \qquad (12)$$

In this study, the energy function (E) is defined as

$$E = \frac{1}{r}\sum_{i=1}^{r}\frac{1}{2}e_i^2 \qquad (13)$$

$$e = \left(\hat{\alpha}_c - \alpha_c^*\right) \qquad (14)$$

where, r is the length of the input pattern, The weights (W_m), dilation (d_{km}) and translation (t_{km}) factors can be updated in accordance with the gradient descent method as shown below.

$$W_m(t+1) = W_m(t) - \eta\frac{\partial e}{\partial W_m}$$
$$t_{km}(t+1) = t_{km}(t) - \eta\frac{\partial e}{\partial t_{km}} \qquad (15)$$
$$d_{km}(t+1) = d_{km}(t) - \eta\frac{\partial e}{\partial d_{km}}$$

5. Determination of The Critical Firing Angle using Neuro-Wavelet Network

The training structure for this works is shown in Fig. 10 (Bilgin, 2008).

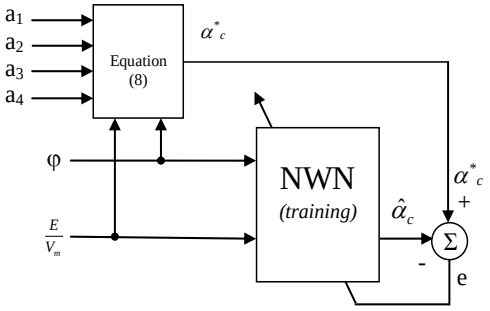

Figure 10. The training structure of NWN.

The inputs of NWN are φ and, E/V_m. The output is critical firing angel α_c. Three neuron is used at mother wavelet layer for each input variable and the three multiplication operator is used wavelet layer. The training pattern is generated from Eq.8. φ is changed from 0,2 to 1 (per-unit) and E/V_m is changed from zero to 0,94 (per-unit) for the training pattern. The NWN is learned with these data until the sum square error is 10^{-6}. The learning pattern and learning result is shown in Fig. 11.

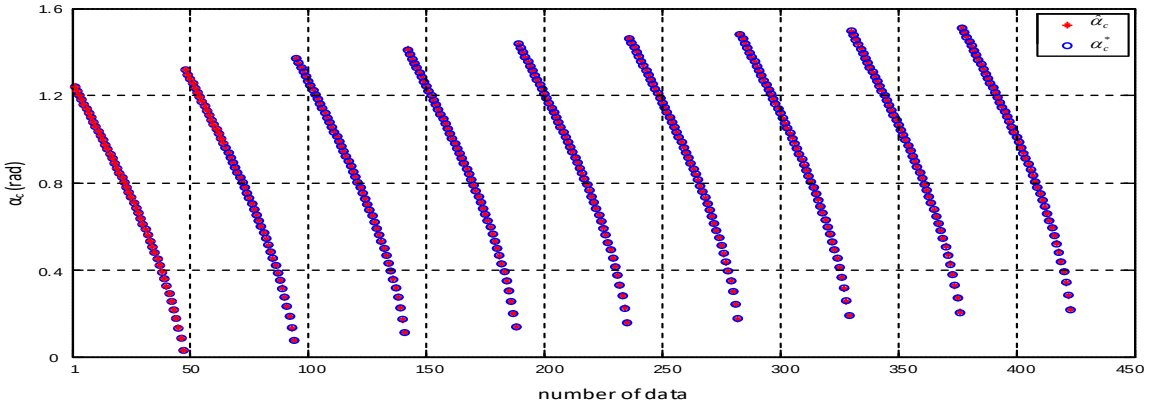

Figure 11. The learning results of NWN

The data is increased and applied to network for learning test. The performance of network is determined with all possible data. The test data and errors is shown in Fig.12.

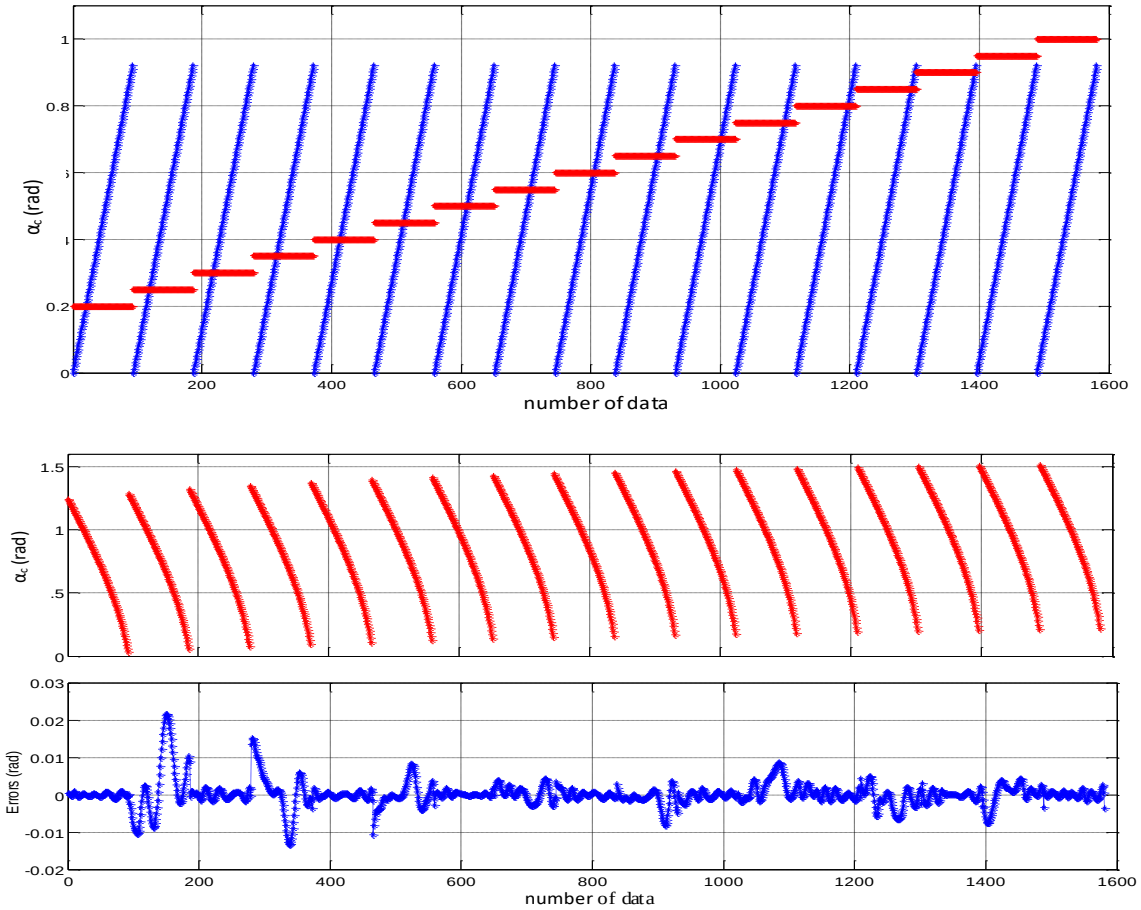

Figure 12. The test result of the trained NWN.

At the end of the learning procedure, the NWN is tested with the new data, which are except the learning pattern. The drive system shown in Fig. 4 was modeled and simulated in MATLAB, and NWN controller performance is obtained. The motor and converter parameters are given in Table 1.

Table 1. Similation Parameters of DC Drive System

Parameter	Value	Paramete	Value
$\mathbf{R_a}$	10Ω	$\mathbf{T_L}$	3 Nm
$\mathbf{L_a}$	0.01 H	$\mathbf{V_m}$	173.2 V
J	0.0165 Kg-m^2	$\mathbf{K_b}$	0.8 V/(rad/sec)
B	0.01 Nm/(rad/sec)	$\mathbf{f_s}$	50 Hz

The simulation results are given in Fig.13 and Fig.14. In Fig. 13, the E/V_m is 0.33 and the φ is variable. In Fig. 14, φ is 0,55 and E/V_m is variable. And φ and E/V_m are variable in Fig. 15.

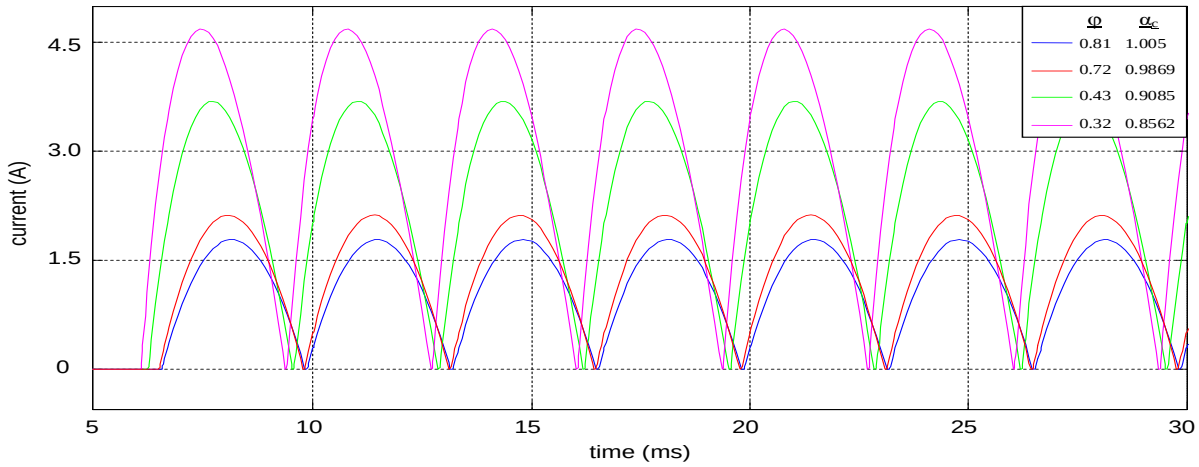

Figure 13. Simulation results of the system with E/V_m=0.33.

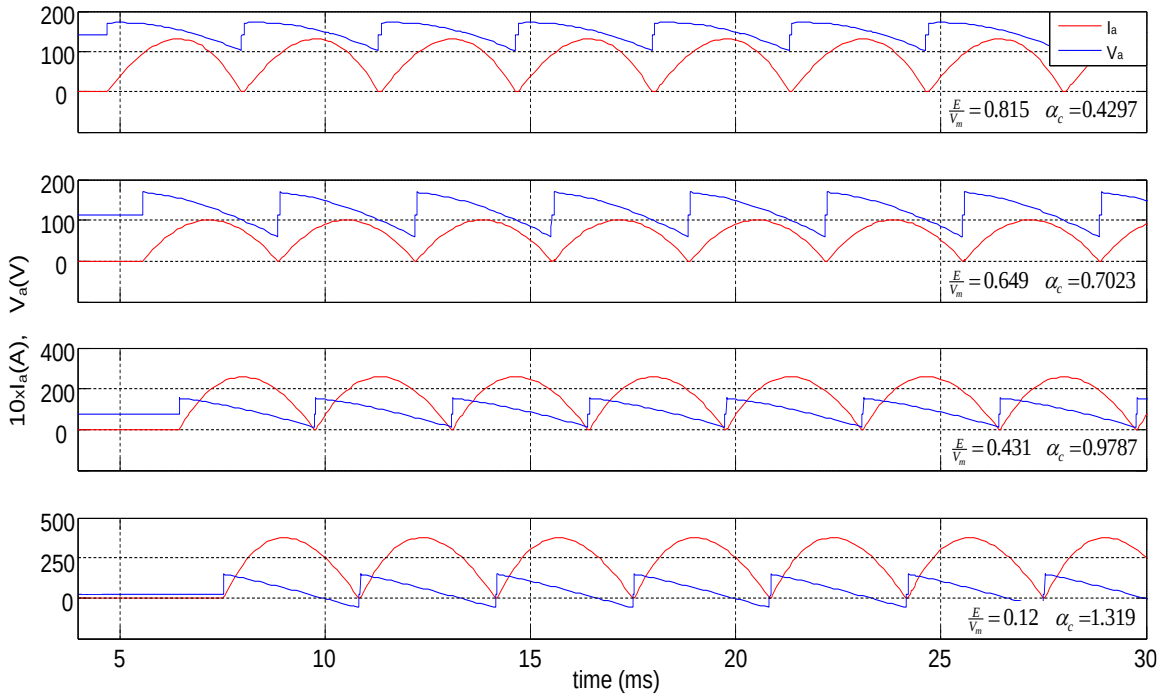

Figure 14. Simulation result of the system, φ=0.55 and various value of E/V_m.

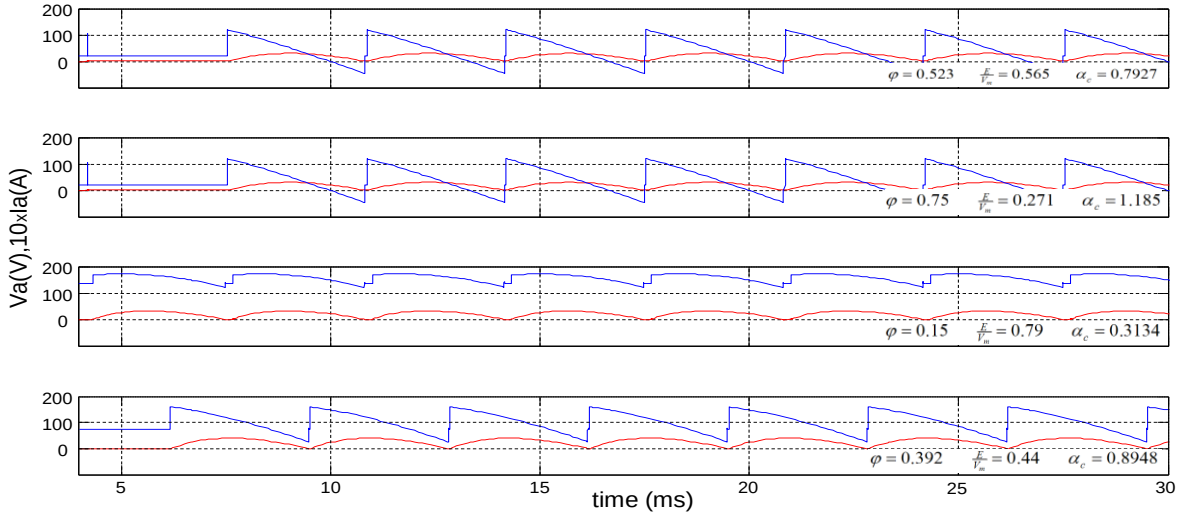

Figure 15. Simulation result of the system with various value of E/V_m and φ.

The various input patterns were entered to NWN and the derived critical firing angle by the NWN was applied to DC motor drive system, which is modeled in MATLAB. The current waveform is examined with all the test inputs. From the simulation results, it can be seen that the NWN controller has determined the critical firing angle precisely.

6. Conclusion

The study presented in this paper has proposed a Neuro-Wavelet Network based critical firing angle determination method for separately exited DC motor drive system fed by three phase controlled rectifier. The simulation results show that, the NWN controller determines the critical firing angle of the converter precisely. Since the critical firing angle calculation is set on per-unit variable, the NWN controller can be used to calculate the ac for any motor drive system. Since the result is produced by NWN at one cycle, it can be said that the proposed method is fast and has less calculation steps than the an iterative methods.

7. References

Abulafya, N. 1995. Neural Networks for System Identification and Control. Ph.D. Thesis, Imperial College of Science, Technology and Medicine, University of London.

Azman, M.A.H., Aris, J.M. , Hussain, Z., Samat, A.A.A., Nazelan, A.M. 2017. A comparative study of fuzzy logic controller and artificial neural network in speed control of separately excited DC motor. 7th IEEE International Conference on Control System, Computing and Engineering (ICCSCE).

Bilgin, M.Z. 2008. Denetimli Doğrultucu ile Beslenen DC Motor için Kritik Tetikleme Açısının Yapay Sinir Ağı Yardımı ile Belirlenmesi. Çukurova Üniversitesi Mühendislik-Mimarlık Fakültesi 30.Yıl Sempozyumu. 16-17 Ekim, Adana, Turkey.

Dmytro, K., Ivan, T., Andriy, Z., Vasyl, T. 2018. Model of the regional energy efficiency analysis based on the artificial neural networks. XIV-th International Conference on Perspective Technologies and Methods in MEMS Design (MEMSTECH).

Guney, E., Dursun, M., Demir, M. 2017. Artificial neural network based real time speed control of a linear tubular permanent magnet direct current motor. International Conference on Control, Automation and Diagnosis (ICCAD).

Guru, B.S., Hızıroğlu, H.R. 2001. Electric Machinery and Transformers. Oxford Univ. Press.

Hafidz, I. Nofi P.E., Anggriawan, D.O., Priyadi, A., Pumomo, M.H. 2017. Neuro wavelet algortihm for detecting high impedance faults in extra high voltage transmission systems. 2nd International Conference Sustainable and Renewable Energy Engineering (ICSREE).

Isa, H., Elyza, N., Dimas, O.A., Ardyono, P., Mauridhi, H.P. 2017. Neuro wavelet algortihm for detecting high impedance faults in extra high voltage transmission systems. 2nd International Conference Sustainable and Renewable Energy Engineering (ICSREE).

Jiang, C., Chau, K., Liu, C., Han, W. 2017. Time-division multiplexing wireless power transfer for separately excited DC motor drives. IEEE Inter. Magnetics Conf. (INTERMAG).

Joshi, M.C., Samanta, S., Srungavarapu, G. 2017. Battery ultracapacitor based DC motor drive for electric vehicles. nIEEE Region 10 Symposium (TENSYMP).

Karas, P., Kozák, Š. 2018. Highly nonlinear process model using optimal artificial neural network. Cybernetics & Informatics (K&I), 1 – 7

Khan, M.A.S.K., Rahman, M.A. 2010. A Novel Neuro-Wavelet-Based Self Tuned Wavelet Controller for IPM Motor Drives. IEEE Transactions on Industry Applications, 46(3), 1194-1203.

Khosravi, M., Heshmatian, S., Khaburi, D.A., Garcia, C., Rodriguez, J. 2017. A novel hybrid model-based MPPT

algorithm based on artificial neural networks for photovoltaic applications. IEEE Southern Power Electronics Conference (SPEC).

Kumar, V.S., Prasad J., Narasimhan, V.L., Ravi, S. 2017. Application of artificial neural networks for prediction of solar radiation for Botswana. International Conference on Energy, Communication, Data Analytics and Soft Computing (ICECDS).

Kundu, S., Chatterjee, D., Chakrabarty, K. 2017. Effect of smoothing reactor on the performance of a PWM chopper fed Dc motor drive. IEEE Calcutta Conference (CALCON).

Kurnia, D.W., Kautsar, S., Etikasari, B., Khafidurrohman, A. 2017. A control scheme for typist robot using Artificial Neural Network. International Conference on Sustainable Information Engineering and Technology (SIET).

Krishnan, R. 2001. Electric Motor Drives. Prentice Hall.

Nahavandi, R., Asadi M., Vazini, H.H. 2018. Improving performance of sensorless vector control using artificial neural network against parametric uncertainty. IEEE 12th International Conference on Compatibility, Power Electronics and Power Engineering (CPE-POWERENG).

Naresh, M., Triphati, R.K. 2016. Power flow control and implementation of PFC rectifier for DC motor drive. IEEE 7th Power India International Conference (PIICON).

Lin, C.M., Hung, K.N., Hsu, C.F. 2007. Adaptive Neuro-Wavelet Control for Switching Power Supplies. IEEE Transactions on Power Electronics, 22(1), 87-95.

Lin, F.J., Wai, R.J., Huang, P.K. 2004. Two-axis Motion Control System Using Wavelet Neural Network for Ultrasonic Motor Drives. IEE Proceedings-Electric Power Applications, 151(5), 613-621.

Lin, C.L., Shieh, N.C. and Tung, P.C. 2002. Robust wavelet neuro control for linear brushless motors. IEEE Transactions on Aerospace and Electronic Systems , 38(3), 918–932.

Omidvar, O., Elliott, D.L. 1997. Neural Systems for Control. New York: Academic Press.

Narendra, K.S., Campagna, D.P. 1990. Identification and Control of Dynamical Systems Using Neural Networks. IEEE Transactions on Neural Networks, 1(1).

Parasuraman, K., Elshorbagy, A. 2005. Wavelet Networks: An Alternative to Classical Neural Networks. Proceedings of International Joint Conference on Neural Networks. Montreal, Canada.

Popov, A.V., Sayarkin, K.S., Zhilenkov, A.A. 2018. Analysis of perspective models of artificial neural networks for control of robotic objects. IEEE Conference of Russian Young Researchers in Electrical and Electronic Engineering (EIConRus).

Prema, V., Jnaneswa, B.S., Badarish, C.A. 2015. Novel training strategies for wavelet-neuro models for wind speed prediction. TENCON 2015 Conference.

Rabiah, B., Saad, D. 2016. Type-II neuro fuzzy wavelet control for power system stability enhancement using STATCOM. 19th International Multi-Topic Conference (INMIC).

Singh, S., Swain, S.C., Dash, R., Roy P. 2017. Current control strategies for SPV grid interconnection based on artificial neural network. Innovations in Power and Advanced Computing Technologies (i-PACT).

Son, T., Nguyen, Phi H.P. 2017. A sensorless three-phase induction motor drive using indirect field oriented control and artificial neural network. 12th IEEE Conference on Industrial Electronics and Applications (ICIEA).

Sridhar, S., K. Uma, R., Sukrutha, J. 2015. Identification of PQ disturbances and degree of loading in induction motor using neuro-wavelets. TENCON 2015 IEEE Reg.10 Conference.

Verma, M., Singh, Agrawal K.K. 2017. Investigation of multiple models of artificial neural networks". International Conference on Intelligent Sustainable Systems (ICISS), 1062-1067.